Kinetic Shock Tubes: Recent Developments for the Study of Homogeneous and Heterogeneous Chemical Processes

Nabiha Chaumeix

Abstract Shock tubes have been successfully used for more than 50 years to study high-temperature chemical kinetics. The main advantages of this ideal reactor are the quasi-instantaneous increase of the temperature and pressure, the absence of mass diffusion, and the clear definition of the initial time. The ability of shock tubes to generate very easily pressures and temperatures over a very large domain (from as low as a few kPa to MPa and from as low as a few hundred Kelvin to several thousands) made them uniquely suitable for various studies from the classical homogeneous autoignition delay times to elementary reaction rate measurements and nanoparticle formation. It has been also used to characterize the shock-to-detonation transition for many chemical systems for propellants such as hydrazine and its derivatives, of light hydrocarbons. The aim of the present paper is to give an overview of different studies related to the kinetics of gaseous and heterogeneous systems with applications related to the chemistry of detonation as well as internal combustion engines. Examples of studies performed at ICARE laboratory as well as in the literature will be given as an illustration.

1 Introduction

The discovery of shock wave existence is due to the pioneer work of Paul Vieille [1], in 1890, on the condition of initiation (and subsequently on failure) of detonation in long tubes. This very important discovery was the experimental proof of their existence about 40 years after Riemann theoretical proposition in 1859 [2] and later by Hugoniot in 1885 [3]. The failure of a detonation initiation led Paul Vieille to report the existence of strong compression waves that travel at supersonic speed and are responsible of a very sharp, instantaneous increase of pressure and temperature. Since it is by nature an irreversible process, the temperature increase is far greater than an isentropic compression for the same pressure ratio. These are the main

N. Chaumeix (✉)
CNRS-INSIS UPR 3021 ICARE Laboratory, Orléans Cedex 2, France
e-mail: chaumeix@cnrs-orleans.fr

A. Sasoh et al. (eds.), *31st International Symposium on Shock Waves 1*,
https://doi.org/10.1007/978-3-319-91020-8_7

features of shock waves that enabled a large variety of studies: an instantaneous pressure and temperature increase with a supersonic shock wave. The shock tube is the device that enables the creation of these shock waves. In these early times, shock tubes were mainly used to study the ignition/failure of detonation waves, and it is only by the end of the 1950s that shock tubes began to be used for chemical kinetics. In the early work of Schott and Kinsley [4], and which was followed by an ever-increasing number of studies based on a similar methodology, the use of highly diluted mixtures to investigate the energy release of the oxidation of hydrogen: the dilution slows down the oxidation process and mitigates the increase of the temperature during the induction period (autoignition delay times). Numerous studies can be found in the literature concerning the measurements of autoignition delay times of a very wide variety of fuels and propellants, usually in the gas phase. The ability to perform experiments with only a few ppm of reactants diluted in a nonreactive gas made the shock tube a very useful device to study elementary reaction rates.

The main advantages of this ideal reactor are the quasi-instantaneous increase of the temperature and pressure, the absence of mass diffusion, and the clear definition of the initial time. The ability of shock tubes to generate very easily pressures and temperatures over a very large domain (from as low as a few kPa to a 100 MPa and from as low as a few hundred Kelvin to several thousands) made them uniquely suitable for various studies from the classical homogeneous autoignition delay times to elementary reaction rate measurements and nanoparticle formation. It has been also used to characterize the shock-to-detonation transition for many chemical systems for propellants such as hydrazine and its derivatives, of light hydrocarbons.

The popularity of shock tubes for chemical kinetic studies relies on the ability of this device to produce, in a very short time, less than a microsecond, any temperature (between 700 K and around 10,000 K) and pressure (0.001–1000 bar). This thermodynamic state pertains generally around a millisecond and is homogeneously distributed during this time with no gradient either of concentration or temperature. These features, which make it an ideal adiabatic reactor, are obtained only if certain conditions are met: the reactive mixture is highly diluted with a monoatomic gas, usually higher than 99%.

The focus of the paper is to illustrate the use of shock tubes in the author's laboratory as well as in the literature. An overview of different studies related to the kinetics of gaseous and heterogeneous systems with applications related to the chemistry of detonation as well as internal combustion engines will be given as an illustration.

2 Shock Tubes Main Features

The principle of shock tubes is based on the use of two connected tubes, usually cylindrical section, separated by a diaphragm. One tube is filled with a high-pressure gas (called driver tube), and the second one is filled with a lower-pressure gas (called

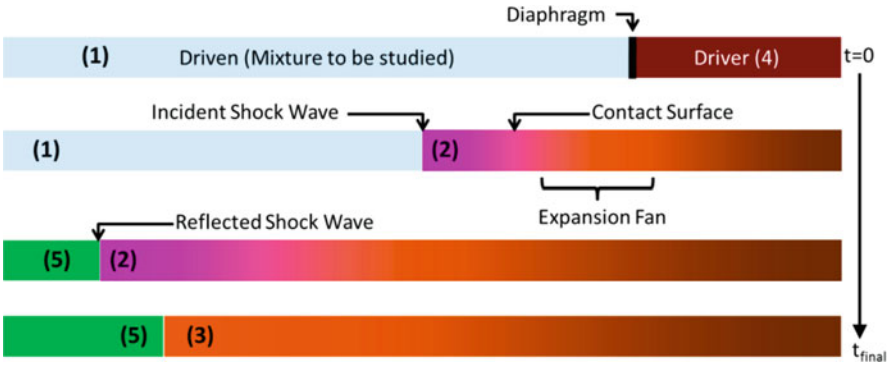

Fig. 1 Schematic of the shock tube principle

driven tube). The rapid destruction of the diaphragm releases the high-pressure gas in the driven tube. The flow of the driver gas will generate a series of compression waves that will rapidly give birth to a normal shock wave that will propagate at supersonic speed in the driven tube ahead of the driver gas flowing in the driven tube. At the same time, an expansion fan is created in the driver gas and will travel in the opposite direction (Fig. 1).

The supersonic incident shock wave hits the endwall of the driven tube and reflects as a shock wave that will be responsible of a second increase of the pressure and temperature of the driven gas. For ideal conditions (normal shock with constant velocity, laminar boundary layer), the medium behind the incident shock acquires a velocity induced by the shock but is brought back to stagnation conditions behind the reflected shock. The thermodynamic conditions behind the incident and the reflected shock waves are easily deduced once the incident shock wave and the thermodynamics of the studied mixture are known. The homogeneous conditions behind reflected shock waves, in terms of pressure and temperature, are maintained during a finite time interval which is defined between the instant of reflection and the time of the arrival of pressure perturbations produced by the interaction of the reflected shock wave and the contact surface (Fig. 2). This time can be increased substantially with tailored conditions. The driver gas composition can be adapted such that the encounter of the reflected shock and the contact surface would not produce pressure waves. Eventually the rarefaction waves will reach the end of the tube and cool down, in a very fast manner, the medium putting an end to the observation time.

Shock tubes have been a very popular tool to study high-temperature chemical kinetic due to two main characteristics: (i) a homogeneous, non-catalytic, stagnated medium which made the assumption of an ideal 0D homogeneous reactor applicable and (ii) the temperature, pressure, and density which are easily deduced from the shock wave Mach number when the thermodynamics of the studied mixture are known.

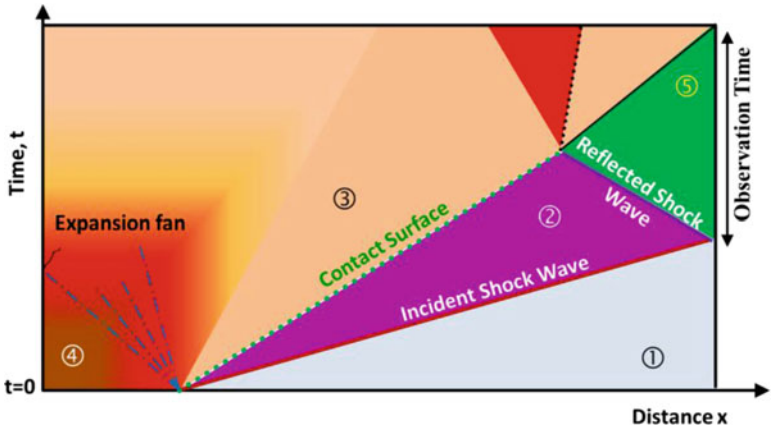

Fig. 2 $x-t$ diagram of an untailored shock wave experiment

Another important feature that has made shock tubes very popular for high-temperature kinetics is the possibility to perform experiments in very highly diluted conditions (usually argon bath) avoiding any temperature change due to exo- or endothermicity subsequently with no effect on the structure or the stability of the wave. The initiation chemistry is often dominated by a limited number of reactions facilitating the analysis of the data from a kinetic point of view.

3 Soot Formation Behind Shock Waves

The formation of soot has been extensively studied over the last decade and is still an extensive research area despite more than a century of studies [5]. Legislation concerning pollutant emissions is more and more stringent in the road transportation sectors of many countries, and soot is one of the targets. To reduce soot particle emissions from vehicles and meet the requirements of the legislation, several methods, often complementary, can be employed. One can mention improvements of the engine technology (e.g., fuel injection system), changes to the aftertreatment system, and fuel formulation. Among these methods, fuel formulation presents the advantage of being engine technology independent and, thus, directly applicable to the entire fleet of existing vehicles. Fuel formulation also allows a decrease of the regeneration frequency of the aftertreatment system and of the associated fuel consumption penalty. It is with this goal in mind that soot formation and characteristics have been extensively studied in the author's group. Soot is the product of an incomplete combustion of hydrocarbon fuels. The main features of soot that are directly linked to the kinetics are (i) the time needed to form these particles from the gas phase, (ii) the conversion efficiency (how much from the

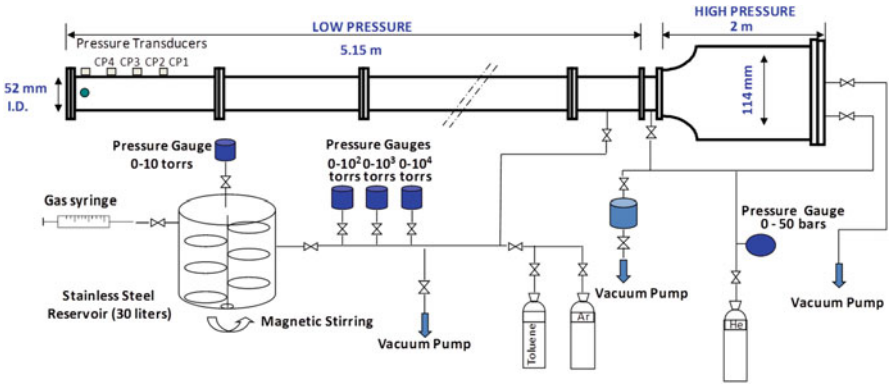

Fig. 3 Schematic of the 52 mm shock tube

initial carbon is actually transformed as soot), (iii) the final size of the soot, (iv) the species adsorbed on soot, and (v) the internal structure and the texture of soot.

Soot formation from the pyrolysis of hydrocarbons behind reflected shock waves will be an ideal configuration to study the effect of different parameters such as temperature, pressure, oxygen content, type of fuels, etc. The shock tube will then be coupled to different diagnostics in order to assess the soot tendency of pure and surrogate fuels. These experiments will be conducted for highly diluted mixtures (>99%).

3.1 The 52 mm Shock Tube at ICARE

The experiments on kinetics of soot formation have been conducted in the 52 mm shock tube. It is a heated stainless steel shock tube (driven section 5.15 m long, 52 mm i.d., driver section 2 m long, 114 mm i.d.) (Fig. 3). The last part of the driven section was equipped with four piezoelectric shock detectors (Chimie Metal, Model A25L05B). These shock detectors have a diameter of 2 mm with a sensitive surface area of 0.75 mm^2 and a rise time of 0.4 μs. The very small surface area coupled with a short rise time allows precise determination of the shock wave passage and, consequently, more accurate evaluation of the temperature and pressure behind the reflected shock wave.

On the other hand, these transducers are very sensitive to heat transfer, and a continuous increase of the signal is observed after the jump due to the passage of the shock waves (Fig. 4). This increase in the signal is due to the limited increase of the gas temperature in the boundary layer, which is sufficient to induce a signal drift that would wrongly lead to the conclusion that the pressure (and hence the temperature) increases strongly immediately behind the reflected shock wave. After this continuous rise in the signal, the end of the observation time is given by the

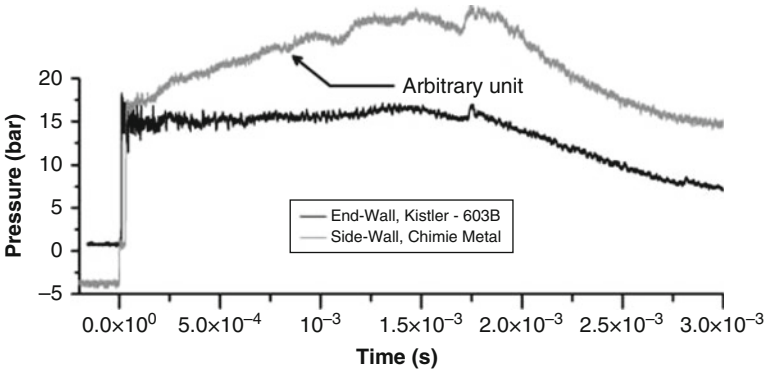

Fig. 4 Comparison between the signals delivered by the Kistler (603B) pressure transducer (black line) and the Chimie Metal shock detector (gray line, in arbitrary units) [6]

decrease of the pressure signal associated with the arrival of the rarefaction waves. Recently, a Kistler pressure transducer (603B) has been installed at the endwall of the shock tube. A comparison of the signal delivered by the two transducers (Chimie Metal on the sidewall location and Kistler on the endwall) during a run with Ar is visible in Fig. 4. As seen, the assumption of constant pressure and temperature behind the reflected shock wave is verified for our highly diluted mixtures.

At the same section as the last transducers, three windows (usually fused silica) are mounted: two are diametrically opposed and the third one at 90° from the others. These windows allow the use of optical diagnostics. To suppress multiple reflections of light, the measurement section was blackened by anodic oxidation over a length of 70 cm. Our setup, under similar conditions, has demonstrated its ability to enable experiments in a well-defined and constant environment, characterized by a flat pressure signal during the 1.5 ms that follow the passage of the RSW [6, 7].

3.2 Diagnostic Techniques for Soot Studies

Several diagnostics have been used with the shock tube to assess the kinetics of soot formation. Laser extinction using different wavelengths: He-Ne laser at 633 nm for most of the studies [6–10] and 810 nm [11]. A schematic of the extinction system is given in Fig. 5.

The laser extinction is applied to measure the soot volume fraction of soot formed from the pyrolysis of a given hydrocarbon. From the transmitted light intensity, soot volume fraction can be inferred if the particles are small enough so that the Rayleigh assumption is fulfilled and the refractive index is known.

The evolution of the soot volume fraction as it varies with time allows the determination of two main important parameters: (i) the soot induction time which is the time needed to build from the gas phase the first solid particles and (ii) the soot

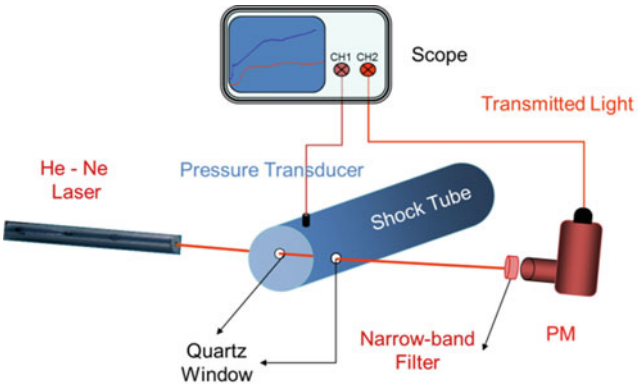

Fig. 5 Laser extinction setup [12]

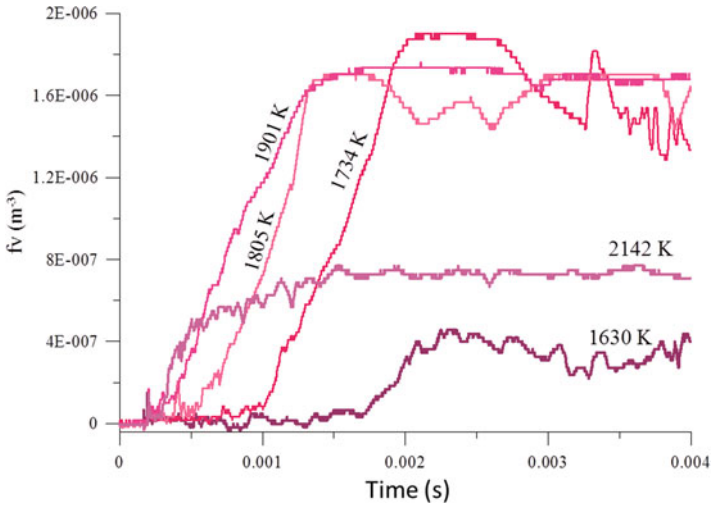

Fig. 6 Soot volume fraction profiles for 0.45% isooctane in argon at P5 around 15 bar [12]

yield which corresponds to the amount carbon that has been effectively transformed to soot. The soot volume fraction profile depends strongly on the temperature (Fig. 6).

From the soot volume fraction evolution, two important characteristics can be deduced: (i) the time needed for the first solid particles to be formed, the induction delay time, decreases strongly with the temperature, and (ii) the soot volume fraction reaches a plateau that depends strongly on the temperature; a maximum amount of soot is formed for a specific temperature (1900 K in case of isooctane). From these measurements, induction delay times and soot yield are deduced.

These experiments rely on the assumption that during the observation time, the soot particles are nano-sized which implicitly assumes that individual spheres are measured and the agglomeration is a late process and takes place during the cooling

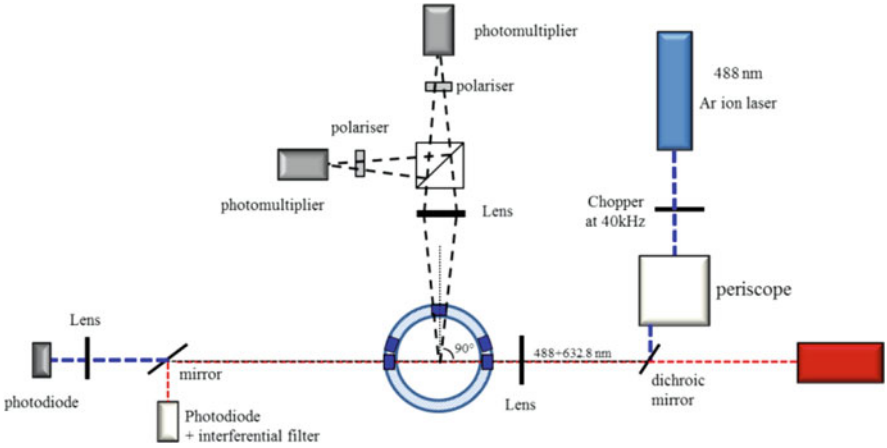

Fig. 7 Experimental setup for scattering/extinction measurements, only at the scattering detection at 90°, is represented [11]

phase of the experiment when the rarefaction waves reach ultimately the end of the shock tube. To do so, a coupled extinction/scattering laser diagnostics have been coupled to the shock tube. A schematic of the optical layout is given in Fig. 7.

The scattered light is measured at three different angles 20°, 90°, and 160°. The ratios between the scattered light at 20° and at 90° on one hand and the ratio 20°/160° on the other hand are a valuable parameter: if the particles scattering the laser light are of Rayleigh size, these ratios are equal to 1, and if any agglomeration takes place, then these ratios will deviate from 1. The ratio as these two different angles is called the dissymmetry ratio. As shown in [11], the dissymmetry ratio deviates from 1 only for times longer than the observation time in the shock tube. These experiments have shown that aggregation can be considered negligible. Subsequently, the formation and growth of a single soot particle can be monitored Fig. 8.

The endwall is a threaded piece which can be dismounted carefully since the soot particles deposit on its surface. Then, it is plunged in a glass of anhydrous ethanol and undergoes a 5 mn cycle of ultrasonic waves. A droplet of the mixture of soot and anhydrous ethanol is deposited on a 3 mm diameter carbon grid (30 μm thick and 400 meshes per inch). The grids are coated with a very thin amorphous carbon supporting film. This film leads to a very low contrast and does not interfere with the soot structure (Fig. 9).

For the high-resolution mode, a holey film was used, the micrographs being taken on soot particles which are across these holes so that no interference between the supporting film and the particle occurs. Several micrographs were taken at two different magnifications:

- 5×104 using the bright-field technique, leading to the primary spheres and the texture

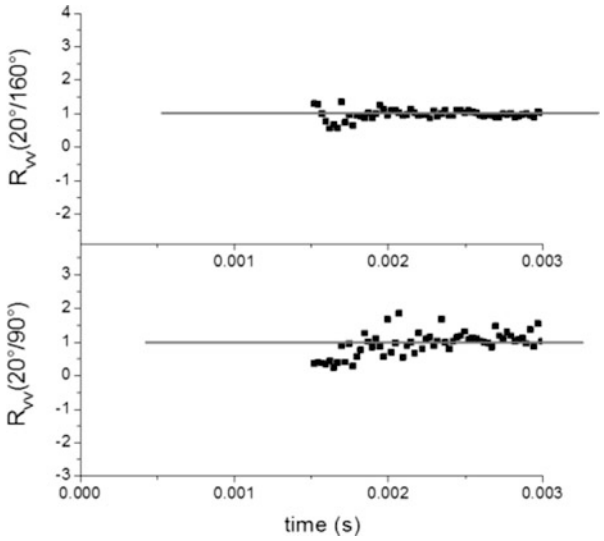

Fig. 8 Dissymmetry ratio for scattered light during the pyrolysis of 2% C_2H_4 in Ar, at 2010 K, and 5.5 bar [11]

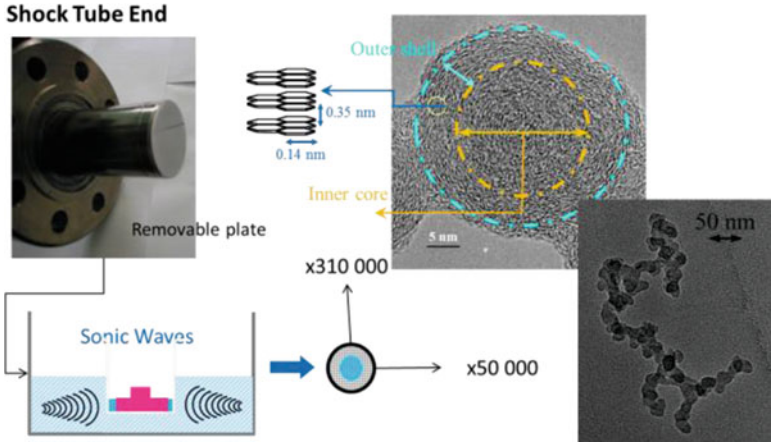

Fig. 9 Soot sampling and TEM analysis. Snaphot of removable end-wall of the shock tube and examples of Soot images obtained by TEM

- 3.1 × 105 using the lattice fringe method, leading to the structure and the micro-texture

Another important parameter from the kinetic point of view is the characterization of the PAHs adsorbed on the soot at the end of the formation process. This investigation was performed by combining laser desorption/ionization time-of-flight mass spectrometry (LDIToFMS) and shock tube experiments. This combination was aimed at the study of adsorbed compounds on aged soot formed at constant

and well-defined temperature. In order to characterize adsorbed species on soot, particles were collected on a polished steel plate (1 mm thickness, 52 mm diameter), maintained on the shock tube's end with a strong magnet. This plate is then directly fixed on a sample holder and introduced in the LDIToFMS without any further preparation. The laser desorption-ionization technique coupled with the time-of-flight mass spectrometer requires a pulsed and focused laser beam to generate ions from adsorbed species on soot. The instrument is equipped with a N2 laser ($\lambda = 337$ nm) (absorption by PAHs negligible). The direct ionization of PAHs without surface modification is obtained using the fourth harmonic of a Nd:YAG laser ($\lambda = 266$ nm). The laser beam is pulsed with an impact diameter of around 20 μm during 4 ns with a constant (±5%) irradiance level estimated between 5 and 10 MW/cm^2. The laser beam's adsorption induces sample heating over a short duration followed by volatilization of adsorbed species. Generated ions are then separated by time-of-flight mass spectrometry. Spectra from LDIToFMS analyses were obtained in positive ion and reflector modes. Since the laser is focused on very small area, either a microscopic variability of sample composition, variations in sample thickness, or imperfect reproducibility of laser-soot interaction is responsible for a poor reproducibility. To overcome it, each spectrum presented here is the sum of 1800 laser shots, collected on the whole end-plate surface (Figs. 10 and 13).

3.3 Main Results on Soot Formation

The main kinetic parameters of soot formation have been determined for heavy pure and surrogate fuels from C3 to C16 hydrocarbons. The induction delay times vary exponentially with the inverse of the temperature (Fig. 11a), the longest delays are

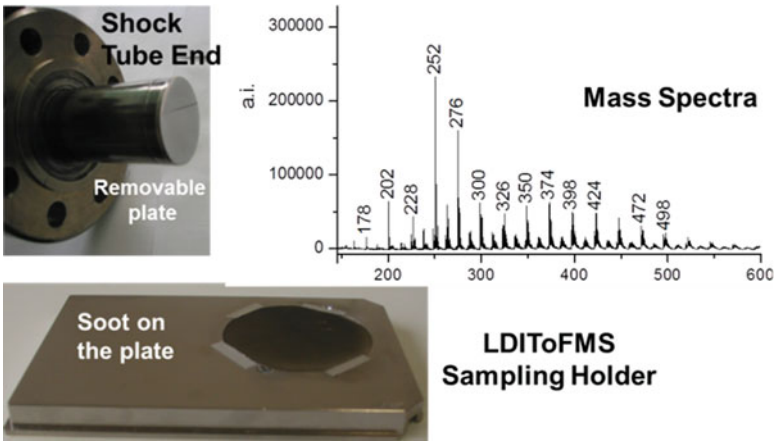

Fig. 10 Soot sampling and TEM analysis [8, 9]. Image of the removable end-wall and of the LDIToFMS sampling holder. Example of a mass spectra follwing soot desoption

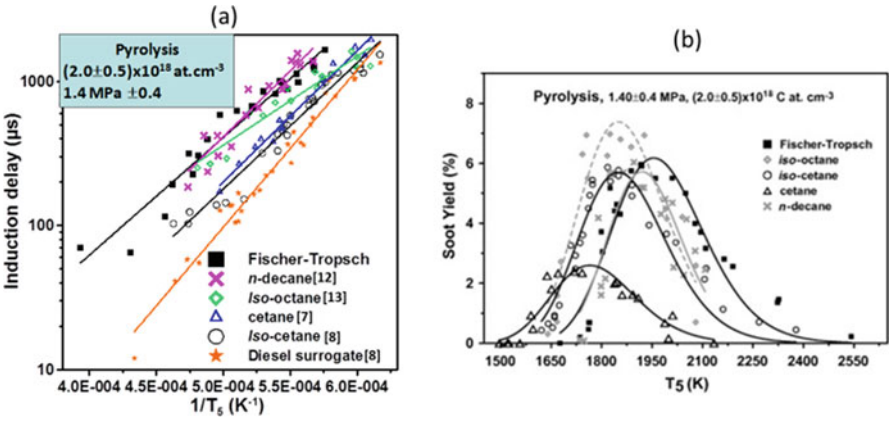

Fig. 11 Fuel propensity for different fuels. (**a**) soot induction delay time versus the inverse reflected shock temperature; (**b**) Soot yield versus the reflected shock temperature. All the mixtures are highly diluted in argon

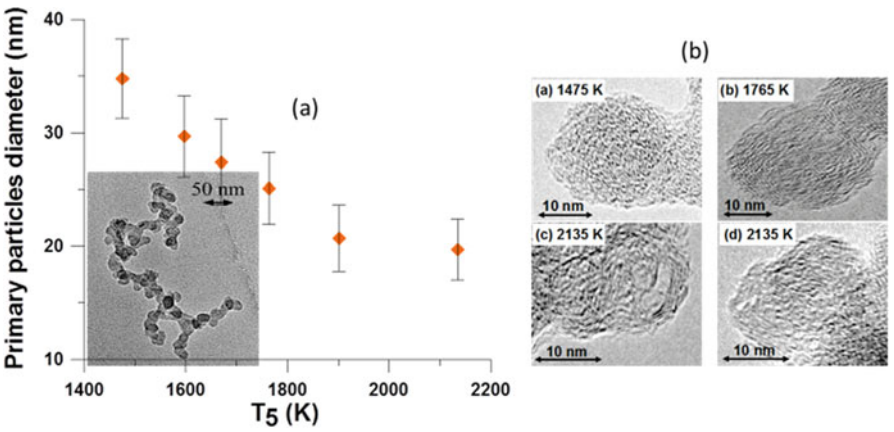

Fig. 12 Soot texture and micro-structure for toluene soot. (**a**) Primary soot particles average diameter versus reflected temperature; (**b**) high resolution of primary soot particls for different temperatures [6–13]

obtained for nonaromatic fuels, and the longest ones are obtained for aromatic fuels. The soot yield exhibits a bell-shaped curve showing the existence of an optimal temperature for which the soot yield is maximum (Fig. 11b).

The TEM analysis showed that the mature soot sampled at the end of each experiment is polydispersed with an average diameter that decreases with the temperature (Fig. 12a). At higher resolution, the measurement of the carbon layers constituting the primary particle spheres shows that the organization of the particle increases with the temperature leading to a more compact structure with longer layers and closely stacked (Fig. 12b).

The MALDI-TOFMS was used to shed light over the species adsorbed at the surface of the soot. A great amount of molecules, which were identified as PAHs, were adsorbed on soot particles. Heavy PAHs were found on soot formed at lower temperatures, while smaller and more compact PAHs appear at higher temperatures. This result agrees well with PAH chemical growth regimes described by Frenklach [14]. Above 1600 K, all major compounds detected were benzenoid PAHs (Fig. 13).

4 Autoignition Delay Times Relevant to Engine Conditions

Autoignition delay times have been measured in shock tubes for decades. The majority of the experiments have been performed in highly diluted conditions and observation times that are limited to around a millisecond. The need for engines that consume less fuel and produce less pollutants at the exhaust led the engine designers to favor leaner combustion regimes at higher pressures. The combination of these two requirements made the engines more sensitive to autoignition delay times with the occurrence of unwanted ignition of the fresh gases during the compression. The severity of these autoignitions is characterized by sharp peak pressure that can lead to the engine destruction. There is a clear need of experimental autoignition delay times for relevant conditions: high pressure (above 20 bar) and for temperatures below 900 °C, which correspond to the negative coefficient temperature. Moreover, these experiments must be performed in air. However, the observation time corresponding to these thermodynamic and non-diluted conditions goes beyond the classical one which highlights then the non-ideal effect of the shock tubes. This non-ideal behavior is responsible for a continuous increase of the pressure behind the reflected shock wave. The Stanford group led by Professor Hanson have investigated these phenomena in details and proposed a method to compensate for the pressure increase and subsequently extend the observation time [15, 16].

This methodology has been successfully applied to the 52 mm shock tube at ICARE to increase the observation time from 1 to more than 4 ms and suppress the non-ideal behavior of the shock tube as it is shown in Fig. 14.

Ignition delay times of several hydrocarbons and oxygenated species have been measured at temperature below 1000 K, and as one can see in Fig. 15, a marked preignition is recorded that is responsible for a substantial increase of the pressure before the main autoignition. This preignition is very sensitive to the temperature. A change by 30 K induces the appearance of the preignition period in the isooctane case. Iso-pentanol exhibits a very marked preignition period with a substantial increase of the pressure during this phase, while the nonreactive profile shows a flat profile (Fig. 15c).

These preliminary results emphasize the importance of the identification of the type of autoignition delay times for these specific thermodynamic conditions that lead to long observation times. The mechanism explaining the preignition is still the focus of ongoing research. The question to be answered is “is it an artefact of the

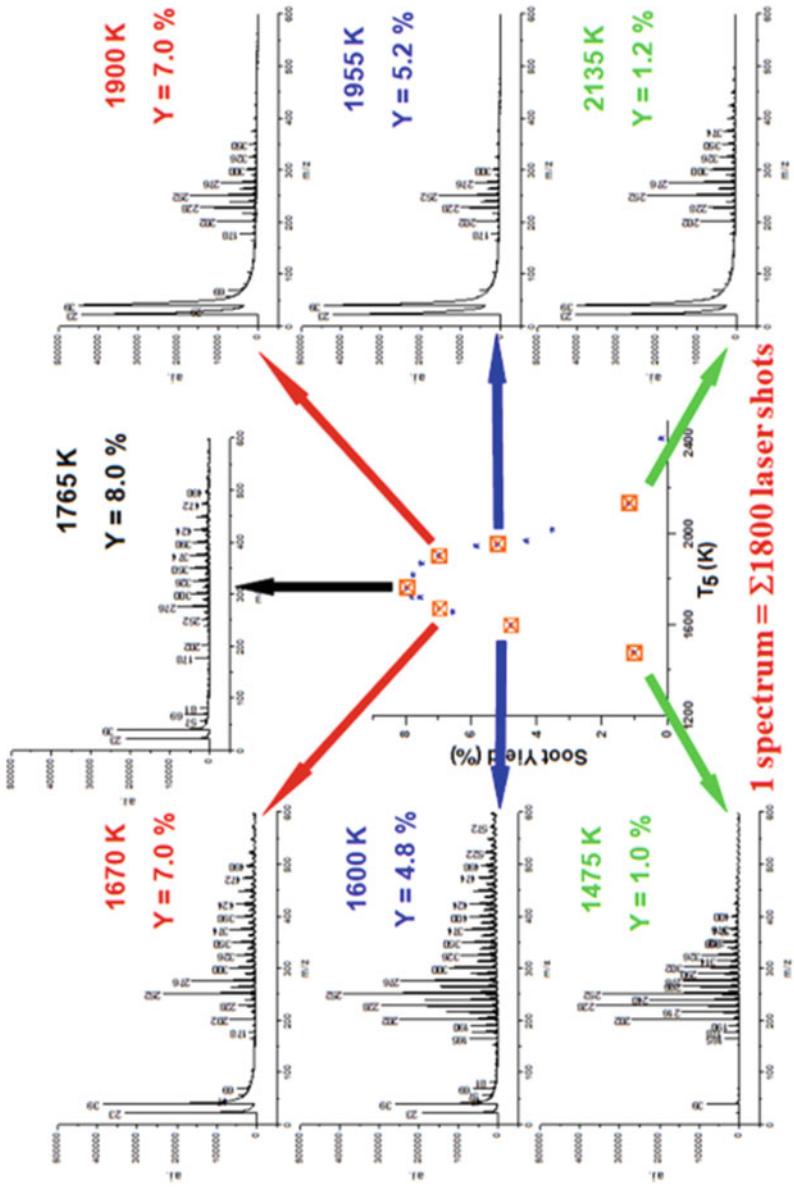

Fig. 13 Absolute intensities of mass spectra obtained by LDITOFMS, soot formed from toluene under pyrolytic conditions [9]

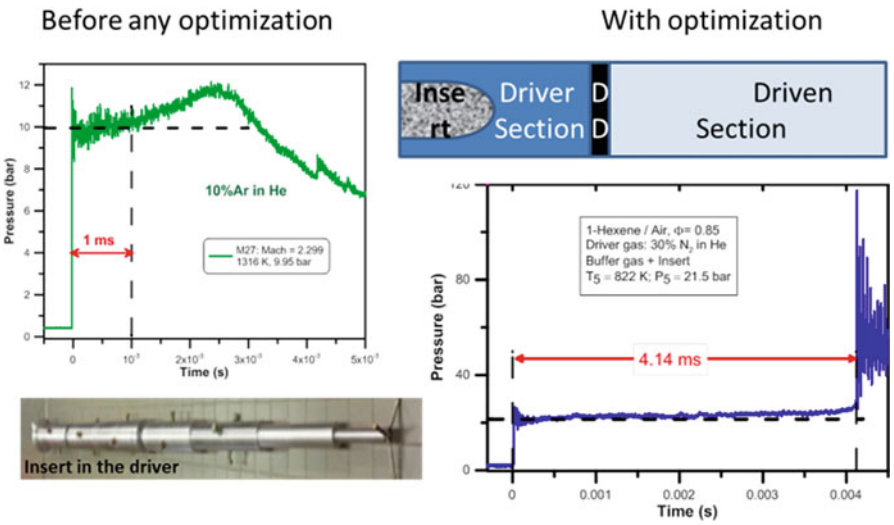

Fig. 14 Pressure profiles in the 52 mm shock tube without and with optimization

shock tube leading to a local ignition such as boundary layer effect, solid particles (from the diaphragm) or from other sources? Or is it related to the chemistry solely." Answering this question is very important as it will bring more understanding not only for internal combustion engine type of studies but also for studies related to shock-to-detonation transition of heavy hydrocarbons [17].

5 Conclusion

The paper describes the use of shock tubes to study soot formation with several diagnostics which help understand the kinetics that are underlined. The use of shock tubes in conditions that are far from the ideal ones is to be done only with special care to take into account for the pressure history and non-ideal effects of the shock tubes. The observation of log delay times proves to be challenging which will require more work before these data can be useful for kinetic analysis.

This paper describes a work that has been and is still being performed by the author's group, and it could not have been done without several fantastic people: Oliver Mathieu, Andrea Comandini, Sylvana de Iuliis, Mahmoud Idir, and Professeur Claude-Etienne Paillard.

The author would like to dedicate this paper to the memory of Professor Paul Roth.

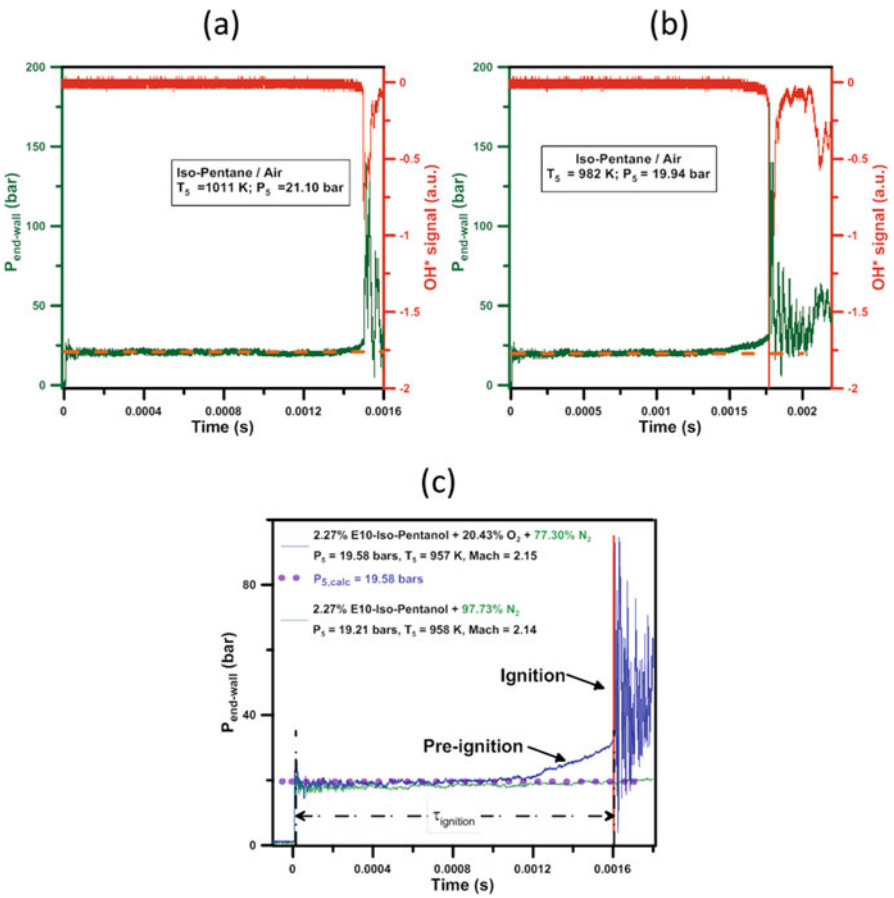

Fig. 15 Identification of different ignition regimes for hydrocarbon/air mixtures around 20bar. (**a**) iso-pentane/air at 1011 K; (**b**) iso-pentane/air at 982 K; (**c**) solid line iso-pentanol/air and dashed-line iso-pentanol/N2 mixtures at 957 K

References

1. P. Vieille, Comptes rendus de l'Académie des Sciences, **111**, 639 (1890)
2. B. Riemann, Abhhandlungen der mathematische Classe des Königlichen Gesellschaft der Wissenschaften zu Göttigen, **8**, 43 (1858–1859)
3. H. Hugoniot, Journal de l'Ecole Polytechnique, 58e cahier, **68** (1889)
4. G.L. Schott, J.L. Kinsley, J. Chem. Phys. **29**, 1177 (1958)
5. W.A. Bone, D.T.A. Townend, (Longmans, Green and Co., New York, 406 1927)
6. O. Mathieu et al., Soot formation from a distillation cut of a Fischer–Tropsch diesel fuel: A shock tube study. Combust. Flame **159**(6), 2192 (2012)
7. F. Douce et al., Soot formation from heavy hydrocarbons behind reflected shock waves. Proc. Combust. Inst. **28**, 2523–2529 (2000)

8. O. Mathieu et al., Experimental study of soot formation from a diesel fuel surrogate in a shock tube. Combust. Flame **156**(8), 1576 (2009)
9. O. Mathieu et al., Characterization of adsorbed species on soot formed behind reflected shock waves. Proc. Combust. Inst. **31**(1), 511 (2007)
10. O. Mathieu et al., Laser desorption–ionization time-of-flight mass spectrometry for analyses of heavy hydrocarbons adsorbed on soot formed behind reflected shock waves. Proc. Combust. Inst. **32**(1), 971 (2009)
11. D. Iuliis et al., Scattering/extinction measurements of soot formation in a shock tube. Exp. Thermal Fluid Sci. **32**(7), 1354 (2008)
12. D. Darius et al., Pyrolysis and oxidation of n-decane, n-propylbenzene and kerosene surrogate behind reflected shock waves, in *Combustion Generated Fine Carbonaceous Particles*, ed. by H. Bockhorn, A. D'Anna, A. F. Sarofim, H. Wang (Eds), (KIT Scientific Publishing, Karlsruhe, 2009), p. 173
13. N. Djebaïli-Chaumeix et al., in *Combustion and Atmospheric Pollution*, ed. by G. D. Roy, S. M. Frolov, A. M. Starik (Torus Press Ltd., Moscow, 2003), p. 411
14. M. Frenklach, Reaction mechanism of soot formation in flames. Phys. Chem. Chem. Phys. **4**, 2028 (2002)
15. Z. Hong et al., Contact surface tailoring condition for shock tubes with different driver and driven section diameters. Shock Waves **19**, 331 (2009)
16. Z. Hong et al., The use of driver inserts to reduce non-ideal pressure variations behind reflected shock waves. Shock Waves **19**, 113 (2009)
17. N. Chaumeix et al., The onset of detonation behind shock waves of moderate intensity in gas phase. Combust. Sci. Tech. **186**(4–5), 607 (2014)